

Practical Differentially Private Hyperparameter Tuning with Subsampling

Antti Koskela and Tejas Kulkarni

Nokia Bell Labs
Espoo, Finland

Abstract

Tuning all the hyperparameters of differentially private (DP) machine learning (ML) algorithms often requires use of sensitive data and this may leak private information via hyperparameter values. Recently, Papernot and Steinke (2022) proposed a certain class of DP hyperparameter tuning algorithms, where the number of random search samples is randomized itself. Commonly, these algorithms still considerably increase the DP privacy parameter ϵ over non-tuned DP ML model training and can be computationally heavy as evaluating each hyperparameter candidate requires a new training run. We focus on lowering both the DP bounds and the computational complexity of these methods by using only a random subset of the sensitive data for the hyperparameter tuning and by extrapolating the optimal values from the small dataset to a larger dataset. We provide a Rényi differential privacy analysis for the proposed method and experimentally show that it consistently leads to better privacy-utility trade-off than the baseline method by Papernot and Steinke (2022).

1 Introduction

Our aim is two-fold: to decrease the computational cost as well as the privacy cost of hyperparameter tuning of DP ML models. The reasons for this are clear. As the dataset sizes grow and models get more complex, blackbox optimization of hyperparameters becomes more expensive since evaluation of a single set of hyperparameters often requires retraining a new model. On the other hand, tuning the hyperparameters often depends on the use of sensitive data, so it requires privacy protection as well, as illustrated by the counterexample by Papernot and Steinke (2022). Intuitively, the leakage from hyperparameters is much smaller than from the model parameters, however providing tuning algorithms with low additional DP cost has turned out challenging. Current best algorithms (Papernot and Steinke, 2022) still come with a considerable DP cost overhead.

Although our methods and results are applicable to general DP mechanisms, we will in particular focus on tuning of the DP stochastic gradient descent (DP-SGD) (Song et al., 2013; Bassily et al., 2014; Abadi et al., 2016) which has become the most widely used method to train ML models with DP guarantees. Compared to plain SGD, DP brings additional hyperparameters to tune: the noise level σ and the clipping constant C . Additionally, also the subsampling ratio γ affects the DP guarantees, as well as length of the training. Tuning all the hyperparameters of DP-SGD commonly requires use of sensitive data.

We use the results by Papernot and Steinke (2022) as building blocks of our methods. Their work was based on the analysis of Liu and Talwar (2019) who provided the first results for DP black-box

optimization of hyperparameters, where, if the base training algorithm is $(\varepsilon, 0)$ -DP, then the tuned model is approximately $(3\varepsilon, 0)$ -DP. Papernot and Steinke (2022) gave Rényi differential privacy (RDP) analysis for a class of black-box tuning algorithms, where the number of random search samples is randomized itself. As the privacy bounds are in terms of RDP and assume only RDP bounds about the candidate model training algorithms, they are particularly suitable to tuning DP-SGD. However, still, running these algorithms increase the ε -values two or three-fold or more, and they can be computationally heavy as evaluating each candidate model requires training a new model. Our novelty is to consider using only a random subset of the sensitive data for the tuning part and use the output hyperparameter values (and potentially the model) for training subsequent models. Using a random subset for the privacy and compute costly part automatically leads to both lower DP privacy leakage as well as computational cost. We also consider ways to appropriately extrapolate the optimal value from the small subset of data to a larger dataset.

The RDP bounds for the DP tuning methods by Papernot and Steinke (2022) assume that the RDP-values of the candidate model training algorithms are fixed. We also consider ways to use these bounds for tuning hyperparameters that affect the RDP-values of the base algorithm, being the noise level σ , the subsampling ratio γ and the length of training in case of DP-SGD.

1.1 Related Work on Hyperparameter Tuning

Chaudhuri and Vinterbo (2013) were the first ones focus on DP bounds for hyperparameter tuning. An improvement was made by Liu and Talwar (2019) who considered black-box tuning of (ε, δ) -DP mechanisms. Mohapatra et al. (2022) showed that for reasonable numbers of adaptively chosen private candidates a naive RDP accounting (i.e., RDP parameters grow linearly w.r.t. number of model evaluations) often leads to lower DP bounds than the methods by Liu and Talwar (2019). Papernot and Steinke (2022) gave RDP bounds for black-box tuning algorithms that grow only logarithmically w.r.t. number of model evaluations. In non-DP setting, hyperparameter tuning with random subsamples has been considered for SVMs (Horváth et al., 2017), for large datasets in healthcare (Waring et al., 2020).. Small random subsets of data have been used in Bayesian optimization of hyperparameters (Swersky et al., 2013; Klein et al., 2017).

1.2 Our Contributions

- We propose a novel subsampling strategy to lower the privacy and compute cost of DP hyperparameter tuning. Our privacy analysis is in terms of RDP and we use existing results for tuning Papernot and Steinke (2022) and DP-SGD (Zhu and Wang, 2019) as building blocks, however our methods and results are independent of those. We provide a tailored RDP analysis for the proposed strategy.
- We propose algorithms to tune hyperparameters that affect the RDP guarantees of the base model training algorithms. We provide a rigorous RDP analysis for these algorithms.
- We carry out experiments on a variety of datasets, where we are able to consistently improve upon the baseline tuning method by a clear margin.

2 Background

2.1 DP and DP-SGD

We first give the basic definitions. An input dataset containing n data points is denoted as $X = (x_1, \dots, x_n) \in \mathcal{X}^n$, where $x_i \in \mathcal{X}$, $1 \leq i \leq n$. We say X and Y are neighbours if we get one by adding or removing one data element to or from the other (denoted $X \sim Y$). Consider a randomized mechanism $\mathcal{M} : \mathcal{X}^n \rightarrow \mathcal{O}$, where \mathcal{O} denotes the output space. The (ε, δ) -definition of DP can be given as follows (Dwork, 2006).

Definition 1. Let $\varepsilon > 0$ and $\delta \in [0, 1]$. We say that a mechanism \mathcal{M} is (ε, δ) -DP, if for all neighbouring datasets X and Y and for every measurable set $E \subset \mathcal{O}$ we have:

$$\Pr(\mathcal{M}(X) \in E) \leq e^\varepsilon \Pr(\mathcal{M}(Y) \in E) + \delta.$$

We will also use the Rényi differential privacy (RDP) (Mironov, 2017) which is defined as follows. Rényi divergence of order $\lambda > 1$ between two distributions P and Q is defined as

$$D_\lambda(P||Q) = \frac{1}{\lambda - 1} \log \int \left(\frac{P(t)}{Q(t)} \right)^\lambda Q(t) dt. \quad (2.1)$$

Definition 2. We say that a mechanism \mathcal{M} is (λ, ε) -RDP, if for all neighbouring datasets X and Y , the output distributions $\mathcal{M}(X)$ and $\mathcal{M}(Y)$ have Rényi divergence of order λ at most ε , i.e.,

$$\max_{X \sim Y} D_\lambda(\mathcal{M}(X)||\mathcal{M}(Y)) \leq \varepsilon.$$

We can convert from Rényi DP to approximate DP using, for example, the following formula:

Lemma 3 (Canonne et al. 2020). Suppose the mechanism \mathcal{M} is (λ, ε') -RDP. Then \mathcal{M} is also $(\varepsilon, \delta(\varepsilon))$ -DP for arbitrary $\varepsilon \geq 0$ with

$$\delta(\varepsilon) = \frac{\exp((\lambda - 1)(\varepsilon' - \varepsilon))}{\lambda} \left(1 - \frac{1}{\lambda} \right)^{\lambda - 1}. \quad (2.2)$$

As is common, in practice we carry out the RDP accounting such that we do bookkeeping of total $\varepsilon(\lambda)$ -values for a list of RDP-orders (e.g. integer λ 's) and in the end convert to (ε, δ) -guarantees by minimizing over the values given by the formula (2.2). RDP accounting for compositions of DP mechanisms is carried using standard RDP composition results (Mironov, 2017).

DP-SGD differs from SGD such that sample-wise gradients of a random mini-batch are clipped to have L_2 -norm at most C and normally distributed noise with variance σ^2 is added to the sum of the gradients of the mini-batch (Abadi et al., 2016). One iteration is given by

$$\theta_{j+1} = \theta_j - \eta_j \left(\frac{1}{|B|} \sum_{i \in B_j} \nabla f(x_i, \theta_j) + Z_j \right), \quad (2.3)$$

where $Z_j \sim \mathcal{N}(\mathbf{0}, \frac{C^2 \sigma^2}{|B|^2} \mathbb{I}_d)$, and η_j denotes the learning rate hyperparameter and $|B|$ is the expected batch size (if we carry out Poisson subsampling of mini-batches, $|B_j|$ varies). There are several RDP results that enable the RDP analysis of DP-SGD iterations (Abadi et al., 2016; Balle et al., 2018; Zhu and Wang, 2019), and nowadays DP-SGD is an indispensable part of frameworks such as Opacus (Yousefpour et al.,

2021) and Tensorflow Privacy (Papernot et al., 2020). The following result by Zhu and Wang (2019) is directly applicable to analyzing DP-SGD, however we also use it for analyzing one of our hyperparameter tuning strategies.

Theorem 4 (Zhu and Wang 2019). *Suppose \mathcal{M} is a $(\lambda, \varepsilon(\lambda))$ -RDP mechanism, w.r.t. to the add/remove neighbourhood relation. Consider the subsampled mechanism $(\mathcal{M} \circ \text{subsample}_{\text{Poisson}(\gamma)})(X)$. If \mathcal{M} is $(\lambda, \varepsilon(\lambda))$ -RDP then $\mathcal{M} \circ \text{subsample}_{\text{Poisson}(\gamma)}$ is $(\lambda, \varepsilon'(\lambda))$ -RDP ($\lambda \geq 2$ is an integer), where*

$$\varepsilon'(\lambda) = \frac{1}{\lambda-1} \log \left((1-\gamma)^{\lambda-1} (\lambda\gamma - \gamma + 1) + \binom{\lambda}{2} \gamma^2 (1-\gamma)^{\lambda-2} e^{\varepsilon(2)} + 3 \sum_{j=3}^{\lambda} \binom{\lambda}{j} \gamma^j (1-\gamma)^{\lambda-j} e^{(j-1)\varepsilon(j)} \right).$$

We remark that the recent works (Koskela et al., 2020; Gopi et al., 2021; Zhu et al., 2022) give methods to carry out (ε, δ) -analysis of DP-SGD tightly.

2.2 DP Hyperparameter Tuning

When tuning the hyperparameters using sensitive data, as Papernot and Steinke (2022) show, private information may leak, especially in case the hyperparameters are chosen based on non-private ML model training. Intuitively, the leakage from hyperparameters is much smaller than from the model parameters, however considering it in the final accounting is essential to ensure rigorous DP guarantees. As described in Section 1.1, currently the most practical (ε, δ) -guarantees for DP hyperparameter tuning algorithms are those of Papernot and Steinke (2022).

In the results of Papernot and Steinke (2022) important is that the number of candidate models K is randomized. They analyze various distributions for drawing K , however we focus on using the Poisson distribution as it is the most concentrated around the mean among all the alternatives. The corresponding hyperparameter tuning algorithm and its privacy guarantees are given as follows.

First recall: K is distributed according to a Poisson distribution with mean $\mu > 0$, if for all non-negative integer values k : $\mathbb{P}(K = k) = e^{-\mu} \cdot \frac{\mu^k}{k!}$.

Theorem 5 (Papernot and Steinke 2022). *Let $Q : \mathcal{X}^N \rightarrow \mathcal{Y}$ be a randomized algorithm satisfying $(\lambda, \varepsilon(\lambda))$ -RDP and $(\hat{\varepsilon}, \hat{\delta})$ -DP for some $\lambda \in (1, \infty)$ and $\varepsilon, \hat{\varepsilon}, \hat{\delta} \geq 0$. Assume \mathcal{Y} is totally ordered. Let the Poisson distribution parameter $\mu > 0$. Define the hyperparameter tuning algorithm $A : \mathcal{X}^N \rightarrow \mathcal{Y}$ as follows. Draw K from a Poisson distribution with mean μ . Run $Q(X)$ for K times. Then $A(X)$ returns the best value of those K runs (both the hyperparameters and the model parameters). If $K = 0$, $A(X)$ returns some arbitrary output. If $e^{\hat{\varepsilon}} \leq 1 + \frac{1}{\lambda-1}$, then A satisfies $(\lambda, \varepsilon'(\lambda))$ -RDP, where*

$$\varepsilon'(\lambda) = \varepsilon(\lambda) + \mu \cdot \hat{\delta} + \frac{\log \mu}{\lambda-1}.$$

Remark 6. *Notice that in a common analysis of DP-SGD, the guarantees hold not only for the best hyperparameters and the corresponding models, but for the whole histories of models: when the output $A(X)$ of the base mechanism is a sequence of DP gradients, post-processing of that sequence gives the sequence of models $(\theta_1, \dots, \theta_T)$. Thus, in the tuning algorithm, we are free to do model checkpointing and choose the best model along the histories.*

3 DP Hyperparameter Tuning with a Random Subset

We next consider our main tools: we carry out the private hyperparameter tuning on a random subset, and if needed, extrapolate the found hyperparameter values to larger datasets that we use for training subsequent models. We consider two strategies: in the first one the subset of data used for tuning is possibly smaller than the data used for training for subsequent models and thus we extrapolate the hyperparameter values. In the other approach, the subsequent models are trained with datasets of the same size as the tuning set.

3.1 Strategy 1: Small Random Subset for Tuning

In the first strategy, we carry out the following steps:

1. Use Poisson subsampling to draw $X_1 \subset X$: draw a random subset X_1 such that each $x \in X$ is included in X_1 with probability q .
2. Compute $(\theta_1, t_1) = \mathcal{M}_1(X_1)$, where \mathcal{M}_1 is a hyperparameter tuning algorithm (e.g., method by Papernot and Steinke, 2022) that outputs the vector of optimal hyperparameters t_1 and the corresponding model θ_1 .
3. If needed, extrapolate the hyperparameters t_1 to the dataset $X \setminus X_1$: $t_1 \rightarrow t_2$.
4. Compute $\theta_2 = \mathcal{M}_2(t_2, X \setminus X_1)$, where \mathcal{M}_2 is the base mechanism (e.g., DP-SGD training run).

Denote the whole mechanism by \mathcal{M} . Then, we may write

$$\mathcal{M}(X) = (\mathcal{M}_1(X_1), \mathcal{M}_2(\mathcal{M}_1(X), X \setminus X_1)). \quad (3.1)$$

Notice that since \mathcal{M}_2 and \mathcal{M}_1 use the same randomness about X_1 , (3.1) cannot be analyzed using standard RDP composition results. We provide a tailored analysis for this method in Section 3.3. However, we can consider alternative third and fourth steps which use the whole dataset X :

3. If needed, extrapolate the hyperparameters t_1 to the dataset X : $t_1 \rightarrow t_2$.
4. Compute $\theta_2 = \mathcal{M}_2(t_2, X)$.

Then, the procedure can be written as a composition

$$\mathcal{M}(X) = (\widehat{\mathcal{M}}_1(X), \mathcal{M}_2(\widehat{\mathcal{M}}_1(X), X)), \quad (3.2)$$

where $\widehat{\mathcal{M}}_1(X) = (\mathcal{M}_1 \circ \text{subsample})(X)$, and the RDP guarantees are obtained using standard subsampling and composition results.

3.1.1 Extrapolating the Hyperparameters

In this work, we use simple heuristics to transfer the optimal hyperparameter values found for the small subset of data to a larger dataset. When using DP-SGD, we use the heuristics used by (van der Veen et al., 2018): we scale the learning rate η with the dataset size. I.e., if we carry out the hyperparameter tuning using a subset of size m and find an optimal value η^* , we multiply η^* by n/m when transferring

to the dataset of size n . Clipping constant C , the noise level σ and the subsampling ratio γ are kept constant in this transfer.

This can be also heuristically motivated as follows. Consider T steps of the DP-SGD (2.3). With the above rules, the distribution of the noise that gets injected into the model is

$$\sum_{j=1}^T Z_j \sim \mathcal{N}\left(0, \frac{T \cdot \left(\frac{n}{m} \eta^*\right)^2 \sigma^2 C^2}{(\gamma \cdot n)^2}\right) \sim \mathcal{N}\left(0, \frac{T \cdot \eta^{*2} \sigma^2 C^2}{(\gamma \cdot m)^2}\right)$$

which is exactly the distribution of the noise added to the model trained with the subsample of size m . Note that such linear scaling of learning rate has also been considered in non-DP SGD (Goyal et al., 2017) to obtain similar validation errors for both small and large minibatch training.

Training of certain models benefits from use of adaptive optimizers such as Adam (Kingma and Ba, 2014) or RMSProp, e.g., due to sparse gradients. Then the above extrapolation rules for DP-SGD are not meaningful anymore. In our experiments, when training a neural network classifier for the IMDB dataset and using Adam with DP-SGD gradients, we found that keeping the value of learning rate fixed in the transfer to the larger dataset lead to better results than increasing it as in case of DP-SGD. We mention that there are principled ways of extrapolating the hyperparameters in non-DP setting such as those of (Klein et al., 2017).

3.2 Strategy 2: Model Ensemble with Disjoint Shards

Strategy 1 can be directly extended to the case, where we divide the dataset into multiple disjoint sets of the same size and train a model for each of the datasets separately. Similar sharding has been considered also in the machine unlearning framework SISA by Bourtole et al. (2021) and also in the framework PATE Papernot et al. (2016) where student models are trained on disjoint datasets. We randomly pick only one of the shards for hyperparameter tuning.

Our strategy 2 is described as follows:

1. Divide X into k shards such that for each data element x of X , the probability of ending up to shard i , $i = 1, \dots, k$, is $1/k$.
2. First compute $(\theta_i, t) = \mathcal{M}_1(X_i)$ using some shard X_i , $i \in [k]$ and then $\theta_j = \mathcal{M}_2(t, X_j)$ for all $j \in [k] \setminus \{i\}$ (can be computed in parallel).
3. Perform predictions using an ensemble of models, i.e., if $f(x, \theta)$ denotes the model output for a data element x with model parameters θ , we carry out predictions using the weighted average $\frac{1}{k} \sum_{j=1}^k f(x, \theta_j)$.

It is reasonable to assume that the optimal hyperparameters for the rest of the shards are not far from those of the shard X_i , i.e., no extrapolation is needed.

3.3 RDP-Analysis of Strategy 1 and Strategy 2

We first consider our strategy 1, i.e., the mechanisms (3.1) and (3.2). The mechanism (3.2) can be analyzed using subsampling and composition results for RDP. Using the RDP values given by Thm. 5 for \mathcal{M}_1 and a subsampling amplification result such as Thm. 4, we obtain RDP bounds for $(\mathcal{M}_1 \circ \text{subsample}_{\text{Poisson}(\gamma)})$. Using RDP bounds for \mathcal{M}_2 (e.g., DP-SGD) and composition results, we further get RDP bounds for \mathcal{M}

of (3.2). However, if we only use the rest of the data $X \setminus X_1$ for \mathcal{M}_2 , i.e. the mechanism (3.1), we can get even tighter RDP bounds.

Let $X \in \mathcal{X}^n$ and $Y = X \cup \{x'\}$ for some $x' \in \mathcal{X}$. To bound the RDP-parameters for the mechanism \mathcal{M} of (3.1), it is sufficient that we find X - and x' -independent bounds for

$$\varepsilon(\lambda) = \max\{D_\lambda(\mathcal{M}(Y)||\mathcal{M}(X)), D_\lambda(\mathcal{M}(X)||\mathcal{M}(Y))\}$$

for different orders of λ . These bounds should be obtained in terms of RDP values for \mathcal{M}_1 (the hyperparameter tuning algorithm, RDP bounds obtained, e.g., using Thm. 5) and for \mathcal{M}_2 (DP-SGD, RDP bounds obtained using, e.g., Thm. 4).

The following theorem gives tailored RDP bounds for the mechanism (3.1). Similarly to the analysis of Zhu and Wang (2019) for the Poisson subsampled Gaussian mechanism, we obtain RDP bounds for (3.1) using the RDP bounds of the mechanisms \mathcal{M}_1 and \mathcal{M}_2 and by using binomial expansions (proof given in the Appendix C.2). We can also use this theorem to analyse the ensemble method described in Section 3.2, since the remaining submodels can be thought of as a parallel composition for which we obtain RDP bounds using Lemma D.1 and its Corollary D.2 of Appendix D.

Theorem 7. *Let $X \in \mathcal{X}^n$ and $Y = X \cup \{x'\}$ for some $x' \in \mathcal{X}$. Let $\mathcal{M}(X)$ be the mechanism described in Section 3.1, such that X_1 is sampled with sampling ratio q , $0 \leq q \leq 1$. Let $\lambda > 1$. Denote by $\varepsilon_P(\lambda)$ and $\varepsilon_Q(\lambda)$ the RDP-values of mechanisms \mathcal{M}_1 and \mathcal{M}_2 , respectively. We have that*

$$\begin{aligned} D_\lambda(\mathcal{M}(Y)||\mathcal{M}(X)) &\leq \frac{1}{\lambda-1} \log \left(q^\lambda \exp((\lambda-1)\varepsilon_P(\lambda)) + (1-q)^\lambda \exp((\lambda-1)\varepsilon_Q(\lambda)) \right. \\ &\quad + \lambda \cdot q^{\lambda-1} \cdot (1-q) \cdot \exp((\lambda-2)\varepsilon_P(\lambda-1)) \\ &\quad + \lambda \cdot q \cdot (1-q)^{\lambda-1} \cdot \exp((\lambda-2)\varepsilon_Q(\lambda-1)) \\ &\quad \left. + \sum_{j=2}^{\lambda-2} \binom{\lambda}{j} \cdot q^{\lambda-j} \cdot (1-q)^j \cdot \exp((\lambda-j-1)\varepsilon_P(\lambda-j)) \exp((j-1)\varepsilon_Q(j)) \right) \end{aligned} \quad (3.3)$$

and

$$\begin{aligned} D_\lambda(\mathcal{M}(X)||\mathcal{M}(Y)) &\leq \frac{1}{\lambda-1} \log \left((1-q)^{\lambda-1} \exp((\lambda-1)\varepsilon_Q(\lambda)) \right. \\ &\quad + q^{\lambda-1} \exp((\lambda-1)\varepsilon_P(\lambda)) \\ &\quad \left. + \sum_{j=1}^{\lambda-2} \binom{\lambda-1}{j} \cdot q^j \cdot (1-q)^{\lambda-1-j} \cdot \exp(j \cdot \varepsilon_P(j+1)) \cdot \exp((\lambda-j-1)\varepsilon_Q(\lambda-j)) \right). \end{aligned} \quad (3.4)$$

Remark 8. *We can initialize the subsequent model training \mathcal{M}_2 using the model θ_1 . This adaptivity is included in the RDP analyses of both strategies (3.1) and (3.2).*

3.4 Computational Savings

The expected number of required gradient evaluation for our strategy 1 is bounded by $\mu \cdot q \cdot n \cdot \text{epochs} + n \cdot \text{epochs}$, whereas the baseline requires in expectation $\mu \cdot n \cdot \text{epochs}$ evaluations. For example, in our experiments with $\mu = 45$ and $q = 0.1$, the baseline method requires $\frac{\mu}{\mu \cdot q + 1} \approx 8$ times more gradient evaluations than our strategy 1.

4 Dealing with Hyperparameters that Affect the DP Guarantees

Theorem 5 gives RDP-parameters of order λ for the tuning algorithm, assuming the underlying candidate picking algorithm is $(\lambda, \varepsilon(\lambda))$ -RDP. If we are tuning, for example, the DP-SGD hyperparameters learning rate η or clipping constant C , and fix rest of the hyperparameters, these $(\lambda, \varepsilon(\lambda))$ -RDP bounds are fixed for all hyperparameter candidates. However, if we tune the hyperparameters that affect the DP guarantees, i.e., the subsampling ratio γ , the noise level σ or the length of the training T , it is less straightforward to determine what are the uniform $\varepsilon(\lambda)$ -upper bounds.

As is common practice, we fix a grid Λ of λ -orders for RDP bookkeeping (e.g. integer values of λ s). If for each random choice of hyperparameters, and for each $\lambda \in \Lambda$, the RDP value $\tilde{\varepsilon}(\lambda)$ of each candidate model is bounded by a value $\varepsilon(\lambda)$, then we can use $\varepsilon(\lambda)$ to obtain RDP-bounds of the hyperparameter tuning algorithm with Theorem 5. This is formally shown below in Lemma 9. For example, when we tune DP-SGD and vary the values of γ and σ , we need to somehow ensure that the RDP values of the candidates stay below the upper bound. We below consider two algorithms for finding random candidates and appropriate upper RDP bounds $\varepsilon(\lambda)$ for the candidate picking algorithm Q .

4.1 Algorithm 1: Grid Search with Randomization

In the first approach we first set an approximative DP target value (ε, δ) which we use to adjust the hyperparameters. For example, if we are tuning the DP-SGD parameters subsampling ratio γ and noise level σ , we can, for each choice of (γ, σ) , adjust the length of the training T so that the resulting training iteration is at most (ε, δ) -DP. Vice versa, we may tune the γ and T , and take minimal value of σ such that the resulting training iteration is at most (ε, δ) -DP.

Consider first tuning of DP-SGD and how to set T for each choice of hyperparameters γ and σ . We first fix $\varepsilon, \delta > 0$ which represent the target approximative DP bound for each candidate model. Denote by $\varepsilon(T, \delta, \gamma, \sigma)$ the approximate DP ε of the subsampled Gaussian mechanism with parameter values γ, σ and T . For each value of (γ, σ) , we attach a number of iterations $T_{\gamma, \sigma}$ such that it is the largest number with which the resulting composition is (ε, δ) -DP:

$$T_{\gamma, \sigma} = \max\{T \in \mathbb{N} : \varepsilon(T, \delta, \gamma, \sigma) \leq \varepsilon\}.$$

As the RDP values increase monotonously w.r.t. number of compositions, it is straightforward to find $T_{\gamma, \sigma}$, e.g., using the bisection method Wang et al. (2019).

Alternatively, we could fix a few values of T , and to each combination of (γ, T) , attach the smallest σ (denoted $\sigma_{\gamma, T}$) such that the target (ε, δ) -bound holds. We prefer this option in our experiments to suit our computational constraints. By the data-processing inequality, the privacy parameters decrease monotonously w.r.t. σ , so that again, e.g., the bisection method can be used to find σ .

We consider a finite grid Γ of possible hyperparameter values t (e.g., in case of DP-SGD, $t = (\gamma, \sigma, T)$, where T is adjusted to γ and σ). Then, for all $t \in \Gamma$, we compute the corresponding RDP value $\varepsilon_t(\lambda)$ for each $\lambda \in \Lambda$. Finally, for each $\lambda \in \Lambda$, we set

$$\varepsilon(\lambda) = \max_{t \in \Gamma} \varepsilon_t(\lambda).$$

Then, for each random draw of t , the DP-SGD trained candidate model is $\varepsilon(\lambda)$ -RDP, and by Lemma 9 below, the candidate picking algorithm Q is also $\varepsilon(\lambda)$ -RDP.

4.2 Algorithm 2: Random Search

Here, we assume we are given some distributions of the hyperparameter candidates and the algorithm Q draws hyperparameters using them. In order to adjust the number of iterations for each candidate, we take a λ -line as an RDP upper bound. More specifically, we require that the candidate models are $(\lambda, c \cdot \lambda)$ -RDP for some $c > 0$ and for all $\lambda \in \Lambda$. Then the number of iterations $T_{\gamma, \sigma}$ for each draw of (γ, σ) is the maximum number of iterations for which the $(\lambda, c \cdot \lambda)$ -RDP bound holds, i.e.,

$$T_{\gamma, \sigma} = \max\{T \in \mathbb{N} : T \cdot \varepsilon_{\gamma, \sigma}(\lambda) \leq c \cdot \lambda \text{ for all } \lambda \in \Lambda\}.$$

Similarly, we can find the minimal σ based on T and γ such that the mechanism is $(\lambda, c \cdot \lambda)$ -RDP for all $\lambda \in \Lambda$.

Again, by Lemma 9 below, the candidate picking algorithm Q is then $c \cdot \lambda$ -RDP and we may use Thm. 5 to obtain RDP bounds for the tuning algorithm

4.3 RDP Analysis of Algorithms 1 and 2

Lemma 9. *Denote by C the random variable of which outcomes are the hyperparameter candidates (drawing either randomly from a grid or from given distributions). Consider an algorithm Q , that first randomly picks hyperparameters $t \sim C$, then runs a randomised mechanism $\mathcal{M}(t, X)$. Suppose $\mathcal{M}(t, X)$ is $(\lambda, \varepsilon(\lambda))$ -RDP for all t . Then, Q is $(\lambda, \varepsilon(\lambda))$ -RDP.*

Proof. Suppose the hyperparameters t are outcomes of a random variable C . Let X and Y be neighbouring datasets. Then, if $p(t, s)$ and $q(t, s)$ (as functions of s) give the density functions of $\mathcal{M}(t, X)$ and $\mathcal{M}(t, Y)$, respectively, we have that

$$Q(X) \sim \mathbb{E}_{t \sim C} p(t, s) \quad \text{and} \quad Q(Y) \sim \mathbb{E}_{t \sim C} q(t, s).$$

Since for any distributions p and q , and for any $\lambda > 1$,

$$\exp((\lambda - 1)D_\lambda(p||q)) = \int \left(\frac{p(t)}{q(t)}\right)^\lambda q(t) dt$$

gives an f -divergence (for $f(x) = x^\lambda$), it is also jointly convex w.r.t. p and q (Liese and Vajda, 2006). Thus, using Jensen's inequality, we have

$$\begin{aligned} \exp((\lambda - 1)D_\lambda(Q(X)||Q(Y))) &= \int \left(\frac{\mathbb{E}_{t \sim C} p(t, s)}{\mathbb{E}_{t \sim C} q(t, s)}\right)^\lambda \cdot \mathbb{E}_{t \sim C} q(t, s) ds \\ &\leq \mathbb{E}_{t \sim C} \int \left(\frac{p(t, s)}{q(t, s)}\right)^\lambda \cdot q(t, s) ds \\ &= \mathbb{E}_{t \sim C} \exp((\lambda - 1)D_\lambda(\mathcal{M}(t, X)||\mathcal{M}(t, Y))) \\ &\leq \mathbb{E}_{t \sim C} \exp((\lambda - 1)\varepsilon(\lambda)) \\ &= \exp((\lambda - 1)\varepsilon(\lambda)) \end{aligned}$$

from which the claim follows. □

4.4 Accuracy of Algorithms 1 and 2

Success of both of these algorithms can be explained by the observation that Poisson subsampled Gaussian mechanism has approximately RDP guarantees of the Gaussian mechanism, i.e., they are actually almost lines w.r.t. the RDP order λ . This is discussed in more detail in Appendix A. For example, as shown in (Thm. 38, Steinke, 2022), if the underlying mechanism is ρ -zCDP, then the Poisson subsampled version with subsampling ratio γ is $(\lambda, 10\gamma^2\rho\lambda)$ -RDP for λ sufficiently small. The larger the value of σ and the smaller the value of γ , the closer the RDPs are to a line, as illustrated in Fig. 3.

5 Experiments

Quality Metric and Evaluation. In all of our experiments, we choose the best model based on the test accuracy. Training and test sets are disjoint, and the quality metric is usually a low sensitivity function. Therefore, even for a private test set, parallel composition can accommodate DP evaluation of a quality metric in the training budget itself. However, we assume that only the training dataset is private and the test data is public for simplicity. This relaxation also allows us to take the best checkpoint over all epochs for each model.

Our plots show the test accuracy of the final model against the final approximate DP ε of the tuning process for several target ε 's, varying from $\{0.4, 0.6, \dots, 2.0\}$. We fix $q = 0.1$ for strategy 1 and $k = 2$ for strategy 2. We mention that in several cases smaller value of q would have lead to better privacy-accuracy trade-off (see Appendix E for additional experiments), however we use the same value $q = 0.1$ in all experiments. The carry out RDP accounting using RDP orders $\{2, \dots, 64\}$ and use $\delta = 10^{-5}$ in all experiments.

Methods. We consider the two variants of strategy 1 in our experiments, one uses the entire dataset X for the final model (green curves, the mechanism (3.2)) and the other uses $X \setminus X_1$ (blue curves, the mechanism (3.1)). The final $\varepsilon(\lambda)$'s for the first and the second version are obtained by combining Thm. 5 with Thm. 4 and Thm. 7, respectively. We expect the first variant to be more accurate for a slightly larger final ε compared to second, since the final models obtained with the mechanism (3.2) use slightly more data than the one obtained with the mechanism (3.1). As discussed in Section 3.1.1, we scale the best learning rate obtained from the first model by the dataset size for training the final model. We do not perform any learning rate scaling in strategy 2 (black curves) because all shards have the same size. In strategy 2, we take the weighted average of the outcomes from both models as the prediction, with weights as the reciprocals of the shard sizes. The method by Papernot and Steinke (2022) described in Thm. 5 is the baseline (red curves).

Datasets and Models. We carry out our experiments on the following standard benchmark datasets for classification: CIFAR-10 (Krizhevsky and Hinton, 2009), MNIST (LeCun et al., 1998), FashionMNIST (Xiao et al., 2017) and IMDB (Maas et al., 2011). For MNIST and IMDB, we use the convolutional neural networks from the examples provided in the Opacus library Yousefpour et al. (2021). For FashionMNIST, we consider a simple feedforward 3-layer ReLU network with hidden layers of width 120. For CIFAR-10, we use a Resnet20 pretrained on CIFAR-100 (Krizhevsky and Hinton, 2009) dataset so that only the last fully connected layer is trained. We minimize the cross-entropy loss in all models. Following the Opacus example, we optimize with DP-Adam for IMDB dataset, but use DP-SGD for others.

Hyperparameters. For these datasets, in one of the experiments we tune only the learning rate, and in the other one the learning rate, batch size, and the number of epochs, while fixing the clipping constant C . The number of trainable parameters and the hyperparameter ranges used are provided in

Table 2 (Appendix B). The numbers of epochs are chosen to suit our computational constraints. Following the procedure from Section 4.1, we compute the smallest σ satisfying a target (ε, δ) bound for each (γ, epoch) pair. The only purpose of target ε ’s is to facilitate the mapping from epochs to σ , and retain comparability across methods.

Initializing with the First Model. We are free to use the first model beyond hyperparameter extraction, since its privacy cost is already accounted for in the privacy analysis. Therefore, we use it to initialize the final model in strategy 1, and the subsequent models in the ensemble in strategy 2.

Implementation. For the implementation of DP-SGD, we use the Opacus library (Yousefpour et al., 2021). For scalability, we explore the hyperparameter spaces with Ray Tune (Liaw et al., 2018) on a multi-GPU cluster. We spell out additional details in the corresponding sections.

5.1 Tuning Learning Rate

The learning rate is among the most critical hyperparameters, and thus we start with a learning rate optimization experiment. We fix the subsampling ratio γ and the number of epochs to the values given in Table 1 (Appendix B) for all models. For example, for $q = 0.1$, $\gamma = 0.0213$ on MNIST dataset, the Poisson subsampling of DP-SGD gives in expectation batch sizes of 128 and 1150 in strategy 1, 640 for strategy 2 with $k = 2$, and 1280 for the baseline method. The learning rate grid size is either 5 or 6, and we use $\mu = 10$, which is sufficiently large to include a good candidate with a large probability.

Plot Description. Figure 1 plots the test accuracy against the final ε for all 4 datasets. The labels with ‘strategy 1’ refer to the mechanism given in (3.1) ($X_1 + X \setminus X_1$) and (3.2) ($X_1 + X$). The label ‘baseline’ refers to the baseline method by (Papernot and Steinke, 2022) described in Thm. 5 and the label ‘strategy 2’ refers to the ensemble method described in Section 3.2. The left panel for each dataset considers the case when the first model output by the tuning algorithm is used to initialize the subsequent model and the right panel shows the results when the first model is not used for initialization. Each plot contains 9 points for each method, one for each target ε ($\varepsilon \in \{0.4, 0.6, \dots, 2.0\}$) for each model training run.

Findings. Our main observation across the board is that the baseline method is generally more accurate for target $\varepsilon \leq 0.5$ (at a much higher final ε), but gets easily matched or outperformed by both variants of strategy 1 for higher target ε ’s. Moreover, as expected, the variant of strategy 1 which uses the entire data in the final model (green plot) performs marginally better than the alternative (blue plot). Strategy 2 is the least accurate method due to lower privacy amplification with subsampling ($q = 0.5$) compared to strategy 1 ($q = 0.1$).

The impact of initializing the final model with the first one on accuracy is not conclusive. For MNIST, FashionMNIST, and CIFAR-10, strategy 2 is slightly more accurate for the same final ε when the model trained on shard 2 is initialized with the first model. For IMDB, however, the opposite is true. Strategy 1 does not seem to then benefit from the initialization either. However, we experimentally observed that the final model achieves its peak accuracy much earlier when initialized with the first model.

5.2 Tuning All Hyperparameters

Next, we also tune the batch size and the number of epochs in addition to the learning rate. The remaining setup is the same as the previous experiment. The choices are listed in Table 2 (Appendix B). Figure 2 shows the same quantities as Figure 1, however higher values of μ are used to accommodate to increased hyperparameter spaces. Strategy 1 is more accurate compared to the baseline for low target ε -values and there is slight degradation in accuracy for higher target ε ’s. For a fixed target ε -value of candidate

models, the final ε -values for strategy 1 are roughly 25 – 30% lower than those of the baseline. We also notice smaller standard errors for CIFAR-10 and FashionMNIST, specially for strategy 2 which might be due to increased chances of finding favorable combinations of hyperparameters. We also note that for final ε -value 2.0, our test accuracies are at least as good as those of (Abadi et al., 2016) in case of MNIST (95% for Abadi et al., 2016) for and approximately the same in case of CIFAR-10 (67% for Abadi et al., 2016), although the results of (Abadi et al., 2016) do not include the DP cost of hyperparameter tuning.

6 Conclusions

We have considered a simple strategy for lowering the privacy and compute cost of DP hyperparameter tuning: we carry out tuning using a random subset of data and extrapolate the optimal values to the larger training set used to train the final model. We have also provided methods to tune the hyperparameters that affect the DP guarantees of the model training themselves, those being the noise level and subsampling ratio in case of DP-SGD. Our experiments show a clear improvement over the baseline method by Papernot and Steinke (2022), when tuning DP-SGD for neural networks and using simple heuristics for the extrapolation. An interesting avenue of future work is to find more sophisticated ways to extrapolate the hyperparameters, something that has been considered in non-DP case (see e.g. Klein et al., 2017).

We have also considered using a weighted ensemble of submodels trained on random disjoint equally-sized subsets of data, in which case extrapolation is not needed. We found it leading to a slightly worse privacy-utility trade-off, albeit with computational speed-ups. Exploring further ways to improve this strategy is also left for future work.

7 Acknowledgments

We would like to thank our colleague Laith Zumot for discussions about practical hyperparameter tuning methods at the initial stages of the project.

Bibliography

- Abadi, M., Chu, A., Goodfellow, I., McMahan, H. B., Mironov, I., Talwar, K., and Zhang, L. (2016). Deep learning with differential privacy. In *Proceedings of the 2016 ACM SIGSAC Conference on Computer and Communications Security*, pages 308–318.
- Balle, B., Barthe, G., and Gaboardi, M. (2018). Privacy amplification by subsampling: Tight analyses via couplings and divergences. In *Advances in Neural Information Processing Systems*, volume 31.
- Bassily, R., Smith, A., and Thakurta, A. (2014). Private empirical risk minimization: Efficient algorithms and tight error bounds. In *2014 IEEE 55th annual symposium on foundations of computer science*, pages 464–473. IEEE.
- Bourtole, L., Chandrasekaran, V., Choquette-Choo, C. A., Jia, H., Travers, A., Zhang, B., Lie, D., and Papernot, N. (2021). Machine unlearning. In *2021 IEEE Symposium on Security and Privacy (SP)*, pages 141–159. IEEE.

- Bun, M. and Steinke, T. (2016). Concentrated differential privacy: Simplifications, extensions, and lower bounds. In *Theory of Cryptography Conference*, pages 635–658. Springer.
- Canonne, C., Kamath, G., and Steinke, T. (2020). The discrete gaussian for differential privacy. In *Advances in Neural Information Processing Systems*, volume 33.
- Chaudhuri, K. and Vinterbo, S. A. (2013). A stability-based validation procedure for differentially private machine learning. *Advances in Neural Information Processing Systems*, 26.
- Dong, J., Roth, A., Su, W. J., et al. (2022). Gaussian differential privacy. *Journal of the Royal Statistical Society Series B*, 84(1):3–37.
- Dwork, C. (2006). Differential privacy. In *Proc. 33rd Int. Colloq. on Automata, Languages and Prog. (ICALP 2006), Part II*, pages 1–12.
- Gopi, S., Lee, Y. T., and Wutschitz, L. (2021). Numerical composition of differential privacy. In *Advances in Neural Information Processing Systems*, volume 34.
- Goyal, P., Dollár, P., Girshick, R., Noordhuis, P., Wesolowski, L., Kyrola, A., Tulloch, A., Jia, Y., and He, K. (2017). Accurate, large minibatch sgd: Training imagenet in 1 hour. *arXiv preprint arXiv:1706.02677*.
- Horváth, T., Mantovani, R. G., and de Carvalho, A. C. (2017). Effects of random sampling on svm hyper-parameter tuning. In *International Conference on Intelligent Systems Design and Applications*, pages 268–278. Springer.
- Kingma, D. P. and Ba, J. (2014). Adam: A method for stochastic optimization. *arXiv preprint arXiv:1412.6980*.
- Klein, A., Falkner, S., Bartels, S., Hennig, P., and Hutter, F. (2017). Fast bayesian optimization of machine learning hyperparameters on large datasets. In *International Conference on Artificial Intelligence and Statistics*, pages 528–536. PMLR.
- Koskela, A., Jälkö, J., and Honkela, A. (2020). Computing tight differential privacy guarantees using FFT. In *International Conference on Artificial Intelligence and Statistics*, pages 2560–2569. PMLR.
- Krizhevsky, A. and Hinton, G. (2009). Learning multiple layers of features from tiny images. Technical Report 0, University of Toronto, Toronto, Ontario.
- LeCun, Y., Bottou, L., Bengio, Y., and Haffner, P. (1998). Gradient-based learning applied to document recognition. *Proceedings of the IEEE*, 86(11):2278–2324.
- Liaw, R., Liang, E., Nishihara, R., Moritz, P., Gonzalez, J. E., and Stoica, I. (2018). Tune: A research platform for distributed model selection and training. *arXiv preprint arXiv:1807.05118*.
- Liese, F. and Vajda, I. (2006). On divergences and informations in statistics and information theory. *IEEE Transactions on Information Theory*, 52(10):4394–4412.
- Liu, J. and Talwar, K. (2019). Private selection from private candidates. In *Proceedings of the 51st Annual ACM SIGACT Symposium on Theory of Computing*, pages 298–309.

- Maas, A., Daly, R. E., Pham, P. T., Huang, D., Ng, A. Y., and Potts, C. (2011). Learning word vectors for sentiment analysis. In *Proceedings of the 49th annual meeting of the association for computational linguistics: Human language technologies*, pages 142–150.
- McSherry, F. D. (2009). Privacy integrated queries: an extensible platform for privacy-preserving data analysis. In *Proceedings of the 2009 ACM SIGMOD International Conference on Management of data*, pages 19–30.
- Mironov, I. (2017). Rényi differential privacy. In *2017 IEEE 30th computer security foundations symposium (CSF)*, pages 263–275. IEEE.
- Mironov, I., Talwar, K., and Zhang, L. (2019). Rényi differential privacy of the sampled Gaussian mechanism. *arXiv preprint arXiv:1908.10530*.
- Mohapatra, S., Sasy, S., He, X., Kamath, G., and Thakkar, O. (2022). The role of adaptive optimizers for honest private hyperparameter selection. In *Proceedings of the AAAI Conference on Artificial Intelligence*, volume 36, pages 7806–7813.
- Papernot, N., Abadi, M., Erlingsson, U., Goodfellow, I., and Talwar, K. (2016). Semi-supervised knowledge transfer for deep learning from private training data. *arXiv preprint arXiv:1610.05755*.
- Papernot, N., Galen, A., and Chien, S. (2020). Tensorflow privacy.
- Papernot, N. and Steinke, T. (2022). Hyperparameter tuning with renyi differential privacy. In *International Conference on Learning Representations*.
- Smith, J., Asghar, H. J., Gioiosa, G., Mrabet, S., Gaspers, S., and Tyler, P. (2022). Making the most of parallel composition in differential privacy. *Proceedings on Privacy Enhancing Technologies*, 1:253–273.
- Song, S., Chaudhuri, K., and Sarwate, A. D. (2013). Stochastic gradient descent with differentially private updates. In *2013 IEEE global conference on signal and information processing*, pages 245–248. IEEE.
- Steinke, T. (2022). Composition of differential privacy & privacy amplification by subsampling. *arXiv preprint arXiv:2210.00597*.
- Swersky, K., Snoek, J., and Adams, R. P. (2013). Multi-task bayesian optimization. *Advances in neural information processing systems*, 26.
- van der Veen, K. L., Seggers, R., Bloem, P., and Patrini, G. (2018). Three tools for practical differential privacy. *NeurIPS 2018 Privacy Preserving Machine Learning workshop*, *arXiv:1812.02890*.
- Van Erven, T. and Harremoës, P. (2014). Rényi divergence and kullback-leibler divergence. *IEEE Transactions on Information Theory*, 60(7):3797–3820.
- Wang, Y.-X., Balle, B., and Kasiviswanathan, S. P. (2019). Subsampled rényi differential privacy and analytical moments accountant. In *The 22nd International Conference on Artificial Intelligence and Statistics*, pages 1226–1235. PMLR.
- Waring, J., Lindvall, C., and Umeton, R. (2020). Automated machine learning: Review of the state-of-the-art and opportunities for healthcare. *Artificial intelligence in medicine*, 104:101822.

- Xiao, H., Rasul, K., and Vollgraf, R. (2017). Fashion-mnist: a novel image dataset for benchmarking machine learning algorithms. Technical report.
- Yousefpour, A., Shilov, I., Sablayrolles, A., Testuggine, D., Prasad, K., Malek, M., Nguyen, J., Ghosh, S., Bharadwaj, A., Zhao, J., et al. (2021). Opacus: User-friendly differential privacy library in pytorch. In *NeurIPS 2021 Workshop Privacy in Machine Learning*.
- Zhu, Y., Dong, J., and Wang, Y.-X. (2022). Optimal accounting of differential privacy via characteristic function. In *International Conference on Artificial Intelligence and Statistics*, pages 4782–4817. PMLR.
- Zhu, Y. and Wang, Y.-X. (2019). Poisson subsampled Rényi differential privacy. In *International Conference on Machine Learning*, pages 7634–7642.

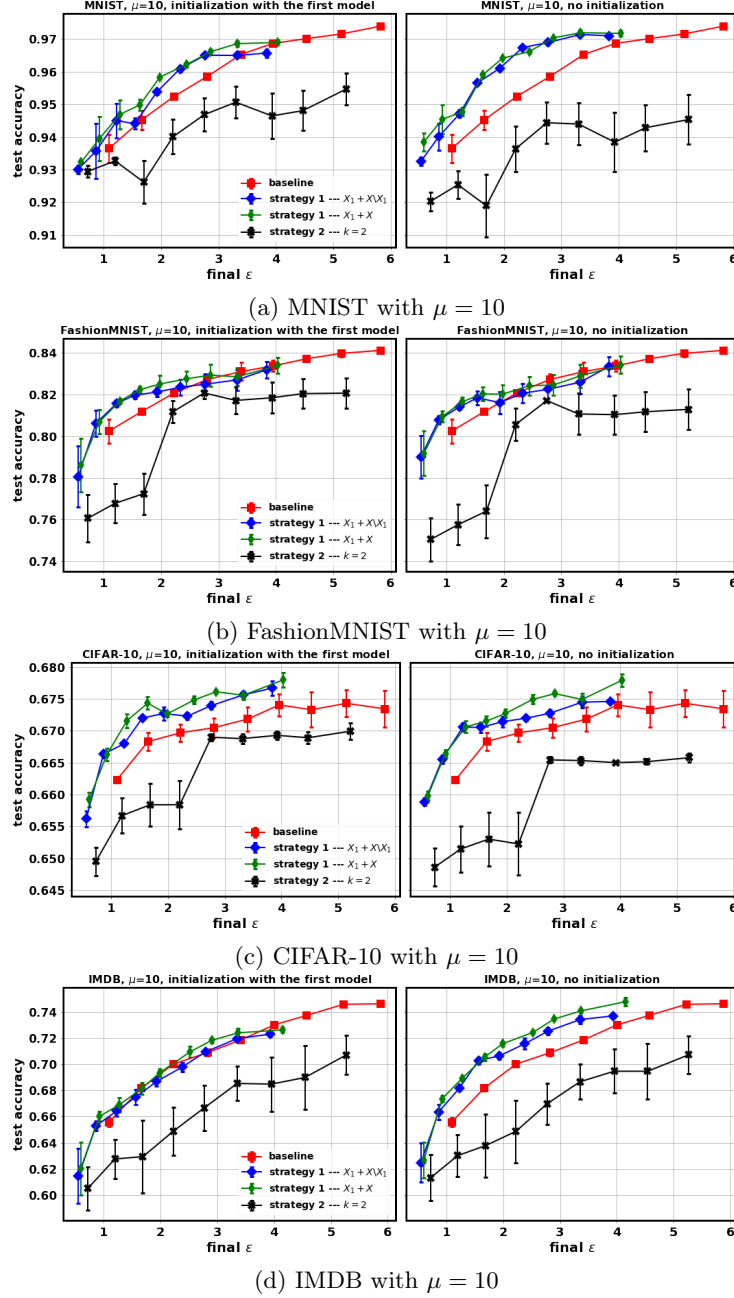


Figure 1: Tuning only the learning rate. Test accuracies averaged across 5 independent runs. The error bars denote the std. error of the mean. Each curve contains 9 points, one for each target $\varepsilon \in \{0.4, 0.6, \dots, 2.0\}$. Here ‘strategy 1’ is ~ 5 times faster than the baseline method by Papernot and Steinke (2022).

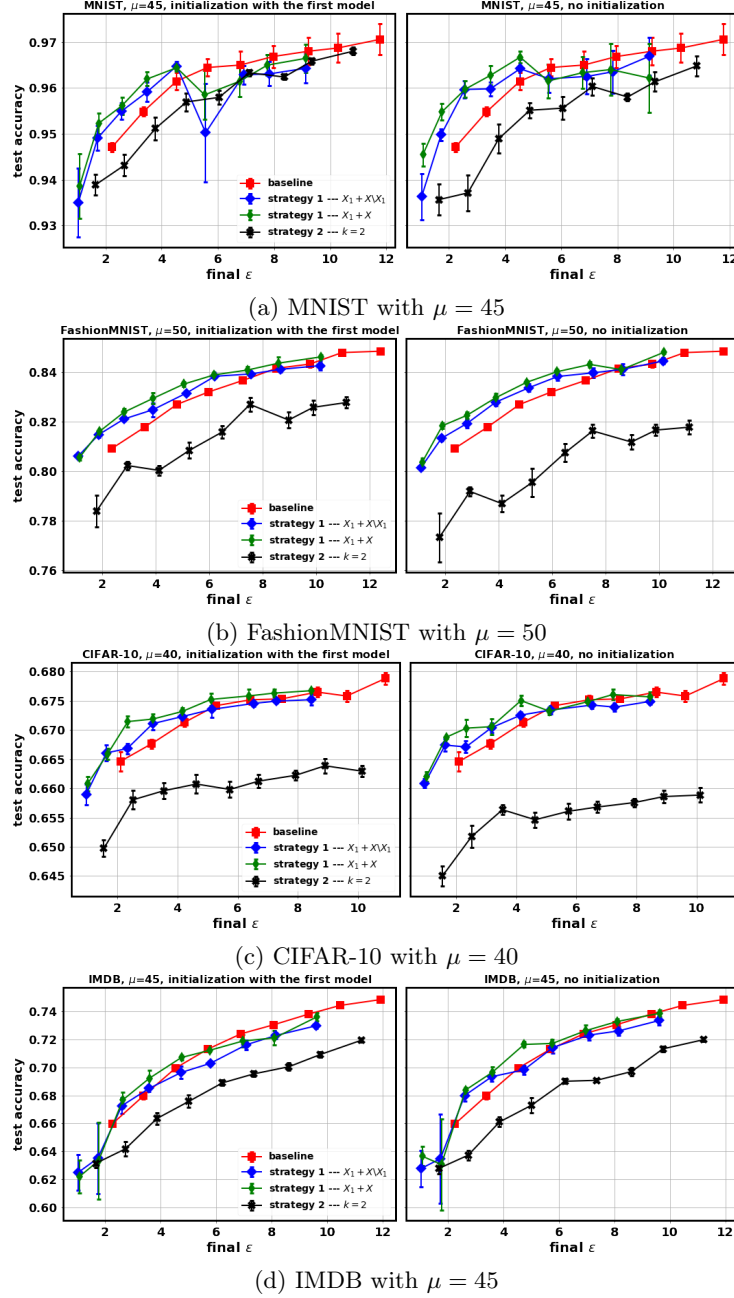


Figure 2: Tuning of subsampling ratio, training length, and learning rate. Test accuracies averaged across 5 independent runs. The error bars denote the std. error of the mean. Each curve contains 9 points, one for each target $\varepsilon \in \{0.4, 0.6, \dots, 2.0\}$. Here 'strategy 1' is ~ 8 times faster than the method by Papernot and Steinke (2022).

Appendix

A Adjusting the Parameters T and σ for DP-SGD

It is often a good approximation to say that the RDP-guarantees of the Poisson subsampled Gaussian mechanism are lines as functions of the RDP order λ , i.e., that the guarantees are those of a Gaussian mechanism with some sensitivity and noise level values. For example, Mironov et al. (Thm. 11, 2019) show that the Poisson subsampled Gaussian mechanism is $(\lambda, 2\gamma^2\lambda/\sigma^2)$ -RDP when λ is sufficiently small. Also, (Thm. 38, Steinke, 2022) show that if the underlying mechanism is ρ -zCDP, then the Poisson subsampled version with subsampling ratio γ is $(\lambda, 10\gamma^2\rho\lambda)$ -RDP when λ is sufficiently small. Notice that the Gaussian mechanism with L_2 -sensitivity Δ and noise level σ is $(\Delta^2/2\sigma^2)$ -zCDP (Bun and Steinke, 2016).

We numerically observe, that the larger the noise level σ and the smaller the subsampling ratio γ , the better the line approximation of the RDP-guarantees (see Figure 3).

In case the privacy guarantees (either (ϵ, δ) -DP or RDP) are approximately those of a Gaussian mechanism with some sensitivity and noise level values, both of the methods for tuning the hyperparameters γ , σ and T described in Section 4 would lead to very little slack. This is because for the Gaussian mechanism, both the RDP guarantees (Mironov, 2017) and (ϵ, δ) -DP guarantees (Dong et al., 2022) depend monotonously on the scaled parameter

$$\tilde{\sigma} = \frac{\sigma}{\Delta \cdot \sqrt{T}}.$$

This means that if we adjust the training length T based on values of σ by having some target (δ, ϵ) -bound for the candidate model (Algorithm 1 of Section 4), the resulting RDP upper bounds of different candidates will not be far from each other (and similarly for adjusting σ based on value of T). Similarly, for Algorithm 2 of Section 4, when adjusting T based on values of σ , the RDP guarantees of all the candidate models would be close to the upper bound ($c \cdot \lambda$, $c > 0$), i.e., they would not be far from each other.

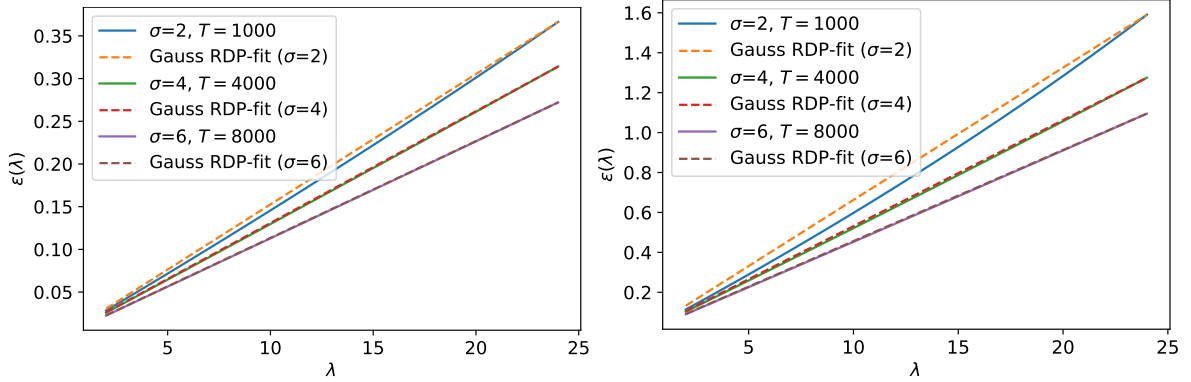


Figure 3: DP-SGD RDP curves for different values of noise level σ and number of compositions T . Left: $\gamma = 1/100$, right: $\gamma = 1/50$ and the corresponding lines with the smallest slope that give upper bounds for the RDP orders up to $\lambda = 24$.

B Hyperparameter Tables for Experiments of Figures 1 and 2

	MNIST	FashionMNIST	CIFAR-10	IMDB
$\gamma = \frac{B}{N}$	0.0213	0.0213	0.0256	0.0256
epochs	40	40	40	110

Table 1: Tuning η : rest of the hyperparameters fixed to these values.

	train/test set	parameters	C	B	learning rate	epochs
MNIST	60k/10k	$\sim 26k$	1	{128, 256}	$\{10^{-i}\}_{i \in \{2, 1.5, 1, 0.5, 0\}}$	{10, 20, 30, 40}
FashionMNIST	60k/10k	$\sim 109k$	3	{128, 256}	$\{10^{-i}\}_{i \in \{2, 1.5, 1, 0.5, 0, -0.5\}}$	{10, 20, 30, 40}
CIFAR-10	50k/10k	0.65k	3	{64, 128}	$\{10^{-i}\}_{i \in \{2, 1.5, 1, 0.5, 0, -0.5\}}$	{20, 30, 40}
IMDB	25k/25k	$\sim 464k$	1	{64, 128}	{0.02, 0.1, 0.2, 1, 1.1}	{50, 70, 90, 110}

Table 2: Tuning σ , η and T : datasets used and the corresponding hyperparameter grids.

C Proof of Theorem 7

C.1 Auxiliary Lemma

We will need the following inequality for the proof of Theorem 7.

Lemma C.1 (Lemma 35, Steinke 2022). *For all $p \in [0, 1]$ and $x \in (0, \infty)$,*

$$\frac{1}{1 - p + \frac{p}{x}} \leq 1 - p + p \cdot x.$$

Remark C.2. *An alternative proof for this result can be obtained using so called Bergström’s inequality, which states that for all $x_k \in \mathbb{R}$, $a_k > 0$, $k \in [n]$,*

$$\frac{(x_1 + \dots + x_n)^2}{a_1 + \dots + a_n} \leq \frac{x_1^2}{a_1} + \dots + \frac{x_n^2}{a_n}. \quad (\text{C.1})$$

In particular, for $n = 2$ and $a_1 = \frac{q}{x}$, $a_2 = 1 - q$, $x_1 = q$, $x_2 = 1 - q$, this gives

$$\frac{1}{1 - q + \frac{q}{x}} \leq 1 - q + q \cdot x.$$

As the proof of Theorem 7 shows, it could be generalized to the case of random k -way split ($k > 2$) using the inequality (C.1).

C.2 Proof of Thm. 7

Proof. We first consider the case $D_\lambda(\mathcal{M}(Y)||\mathcal{M}(X))$. Let $X \in \mathcal{X}^n$ and $x' \in \mathcal{X}$. Denote

$$\varepsilon_1(\lambda) = D_\lambda(\mathcal{M}(X \cup \{x'\})||\mathcal{M}(X)).$$

Looking at Strategy 1 which uses Poisson subsampling with subsampling ratio q to obtain the dataset X_1 , and conditioning the output on the randomness in choosing X_1 , we can write the mechanism as a mixture over all possible choices of X_1 as

$$\mathcal{M}(X) = \sum_{X_1} p_{X_1} \cdot (\mathcal{M}_1(X_1), \mathcal{M}_2(\mathcal{M}(X_1), X \setminus X_1)), \quad (\text{C.2})$$

where p_{X_1} is the probability of sampling X_1 . Since each data element is in X_1 with probability q , we can furthermore write $\mathcal{M}(X \cup \{x'\})$ as a mixture

$$\begin{aligned} \mathcal{M}(X \cup \{x'\}) = \sum_{X_1} p_{X_1} \cdot & \left(q \cdot (\mathcal{M}_1(X_1 \cup \{x'\}), \mathcal{M}_2(\mathcal{M}_1(X_1 \cup \{x'\}), X \setminus X_1)) \right. \\ & \left. + (1 - q) \cdot (\mathcal{M}_1(X_1), \mathcal{M}_2(\mathcal{M}(X_1), X \setminus X_1 \cup \{x'\})) \right). \end{aligned} \quad (\text{C.3})$$

From the quasi-convexity of the Rényi divergence (Van Erven and Harremoës, 2014) and the expressions (C.2) and (C.3), it follows that

$$\begin{aligned} D_\lambda(\mathcal{M}(X \cup \{x'\})||\mathcal{M}(X)) \leq & \sup_{X_1} D_\lambda(q \cdot (\mathcal{M}_1(X_1 \cup \{x'\}), \mathcal{M}_2(\mathcal{M}_1(X_1 \cup \{x'\}), X \setminus X_1)) \\ & + (1 - q) \cdot (\mathcal{M}_1(X_1), \mathcal{M}_2(\mathcal{M}(X_1), X \setminus X_1 \cup \{x'\})) || (\mathcal{M}_1(X_1), \mathcal{M}_2(\mathcal{M}(X_1), X \setminus X_1))). \end{aligned} \quad (\text{C.4})$$

Our aim is to express the right-hand side of (C.4) in terms of RDP parameters of \mathcal{M}_1 and \mathcal{M}_2 . To this end, take an arbitrary $X_1 \subset X$, and denote by

- $\tilde{P}(t)$ the density function of $\mathcal{M}_1(X_1 \cup \{x'\})$,
- $P(t)$ the density function of $\mathcal{M}_1(X_1)$,
- $\tilde{Q}(t, s)$ the density function of $\mathcal{M}_2(t, X \setminus X_1 \cup \{x'\})$ for auxiliary variable t (the output of \mathcal{M}_1),
- $Q(t, s)$ the density function of $\mathcal{M}_2(t, X \setminus X_1)$ for auxiliary variable t .

Then, we see that

$$\mathbb{P}((\mathcal{M}_1(X_1), \mathcal{M}_2(\mathcal{M}(X_1), X \setminus X_1)) = (t, s)) = P(t) \cdot Q(t, s)$$

and similarly that

$$\begin{aligned} \mathbb{P}(q \cdot (\mathcal{M}_1(X_1 \cup \{x'\}), \mathcal{M}_2(\mathcal{M}_1(X_1 \cup \{x'\}), X \setminus X_1)) & + (1 - q) \cdot (\mathcal{M}_1(X_1), \mathcal{M}_2(\mathcal{M}(X_1), X \setminus X_1 \cup \{x'\})) = (t, s)) \\ = q \cdot \mathbb{P}((\mathcal{M}_1(X_1 \cup \{x'\}), \mathcal{M}_2(\mathcal{M}_1(X_1 \cup \{x'\}), X \setminus X_1)) & = (t, s)) \\ + (1 - q) \cdot \mathbb{P}((\mathcal{M}_1(X_1), \mathcal{M}_2(\mathcal{M}(X_1), X \setminus X_1 \cup \{x'\})) & = (t, s)) \\ = q \cdot \tilde{P}(t) \cdot \tilde{Q}(t, s) + (1 - q) \cdot P(t) \cdot Q(t, s). \end{aligned}$$

By the definition of the Rényi divergence, we have that

$$\begin{aligned}
& \exp \left((\lambda - 1) D_\lambda (q \cdot (\mathcal{M}_1(X_1 \cup \{x'\}), \mathcal{M}_2(\mathcal{M}_1(X_1 \cup \{x'\}), X \setminus X_1)) \right. \\
& \quad \left. + (1 - q) \cdot (\mathcal{M}_1(X_1), \mathcal{M}_2(\mathcal{M}(X_1), X \setminus X_1 \cup \{x'\})) || (\mathcal{M}_1(X_1), \mathcal{M}_2(\mathcal{M}(X_1), X \setminus X_1))) \right) \\
& = \int \int \left(\frac{q \cdot \tilde{P}(t) \cdot Q(t, s) + (1 - q) \cdot P(t) \cdot \tilde{Q}(t, s)}{P(t) \cdot Q(t, s)} \right)^\lambda \cdot P(t) \cdot Q(t, s) \, dt \, ds.
\end{aligned} \tag{C.5}$$

which can be expanded as

$$\begin{aligned}
& \int \int \left(\frac{q \cdot \tilde{P}(t) \cdot Q(t, s) + (1 - q) \cdot P(t) \cdot \tilde{Q}}{P(t) \cdot Q(t, s)} \right)^\lambda P(t) \cdot Q(t, s) \, dt \, ds \\
& = \int \int \left(q \cdot \frac{\tilde{P}(t)}{P(t)} + (1 - q) \cdot \frac{\tilde{Q}(t, s)}{Q(t, s)} \right)^\lambda P(t) \cdot Q(t, s) \, dt \, ds \\
& = \int \int q^\lambda \left(\frac{\tilde{P}(t)}{P(t)} \right)^\lambda P(t) \cdot Q(t, s) \, dt \, ds \\
& \quad + \int \int (1 - q)^\lambda \left(\frac{\tilde{Q}(t, s)}{Q(t, s)} \right)^\lambda P(t) \cdot Q(t, s) \, dt \, ds \\
& \quad + \int \int \lambda \cdot q^{\lambda-1} \cdot (1 - q) \cdot \left(\frac{\tilde{P}(t)}{P(t)} \right)^{\lambda-1} P(t) \cdot \tilde{Q}(t, s) \, dt \, ds \\
& \quad + \int \int \lambda \cdot q \cdot (1 - q)^{\lambda-1} \cdot \left(\frac{\tilde{Q}(t, s)}{Q(t, s)} \right)^{\lambda-1} Q(t, s) \cdot \tilde{P}(t) \, dt \, ds \\
& \quad + \int \int \sum_{j=2}^{\lambda-2} \binom{\lambda}{j} \cdot q^{\lambda-j} \cdot (1 - q)^j \cdot \left[\left(\frac{\tilde{P}(t)}{P(t)} \right)^{\lambda-j} P(t) \right] \left[\left(\frac{\tilde{Q}(t, s)}{Q(t, s)} \right)^j Q(t, s) \right] \, dt \, ds.
\end{aligned} \tag{C.6}$$

We next bound the five integrals on the right hand side of (C.6). For the first two integrals, we use the RDP-bounds for \mathcal{M}_1 and \mathcal{M}_2 to obtain

$$\begin{aligned}
\int \int \left(\frac{\tilde{P}(t)}{P(t)} \right)^\lambda P(t) Q(t, s) \, dt \, ds & = \int \int \left(\frac{\tilde{P}(t)}{P(t)} \right)^\lambda P(t) \, dt \\
& \leq \exp((\lambda - 1) \varepsilon_P(\lambda)).
\end{aligned} \tag{C.7}$$

and

$$\begin{aligned}
\int \int \left(\frac{\tilde{Q}(t, s)}{Q(t, s)} \right)^\lambda Q(t, s) P(t) \, ds \, dt & \leq \int \int \exp((\lambda - 1) \varepsilon_Q(\lambda)) P(t) \, dt \\
& = \exp((\lambda - 1) \varepsilon_Q(\lambda)),
\end{aligned} \tag{C.8}$$

where ε_P and ε_Q give the RDP-parameters of order λ for \mathcal{M}_1 and \mathcal{M}_2 , respectively. The third and fourth integral can be bounded analogously. In the second inequality we have also used the fact that the RDP-parameters of \mathcal{M}_2 are independent of the auxiliary variable t . Similarly, for the third integral, we have

$$\begin{aligned} \int \int \left[\left(\frac{\tilde{P}(t)}{P(t)} \right)^{\lambda-j} P(t) \right] \left[\left(\frac{\tilde{Q}(t,s)}{Q(t,s)} \right)^j Q(t,s) \right] ds dt &\leq \int \int \left[\left(\frac{\tilde{P}(t)}{P(t)} \right)^{\lambda-j} P(t) \right] \exp((j-1)\varepsilon_Q(j)) dt \\ &\leq \exp((\lambda-j-1)\varepsilon_P(\lambda-j)) \cdot \exp((j-1)\varepsilon_Q(j)). \end{aligned} \quad (\text{C.9})$$

Substituting (C.7), (C.8) (and similar expressions for the third and fourth integral) and (C.9) to (C.6), we get a bound for (C.5). Since $X_1 \subset X$ was arbitrary, we arrive at the claim via (C.4).

Next, we consider bounding $D_\lambda(\mathcal{M}(X) \parallel \mathcal{M}(Y))$. The proof goes similarly as the one for $D_\lambda(\mathcal{M}(Y) \parallel \mathcal{M}(X))$. Denote

$$\varepsilon_2(\lambda) = D_\lambda(\mathcal{M}(X) \parallel \mathcal{M}(X \cup \{x'\})).$$

With the notation of proof of Thm. 7, we see that, instead of (C.5), we need to bound

$$\begin{aligned} &\exp((\lambda-1)\varepsilon_2(\lambda)) \\ &= \int \int \left(\frac{P(t) \cdot Q(t,s)}{q \cdot \tilde{P}(t) \cdot Q(t,s) + (1-q) \cdot P(t) \cdot \tilde{Q}(t,s)} \right)^\lambda (q \cdot \tilde{P}(t) \cdot Q(t,s) + (1-q) \cdot P(t) \cdot \tilde{Q}(t,s)) dt ds. \end{aligned}$$

In order to use here the series approach, we need to use Lemma C.1:

$$\begin{aligned} &\left(\frac{P \cdot Q}{q \cdot \tilde{P} \cdot Q + (1-q) \cdot P \cdot \tilde{Q}} \right)^\lambda (q \cdot \tilde{P} \cdot Q + (1-q) \cdot P \cdot \tilde{Q}) \\ &= \left(\frac{P \cdot Q}{q \cdot \tilde{P} \cdot Q + (1-q) \cdot P \cdot \tilde{Q}} \right)^{\lambda-1} \cdot P \cdot Q \\ &= \left(q \cdot \frac{\tilde{P}}{P} + (1-q) \cdot \frac{\tilde{Q}}{Q} \right)^{1-\lambda} \cdot P \cdot Q \\ &= \left(q \cdot \frac{\tilde{P} Q}{P \tilde{Q}} + (1-q) \right)^{1-\lambda} \cdot \left(\frac{\tilde{Q}}{Q} \right)^{1-\lambda} \cdot P \cdot Q \\ &= \left(q \cdot \frac{\tilde{P} Q}{P \tilde{Q}} + (1-q) \right)^{1-\lambda} \cdot \left(\frac{Q}{\tilde{Q}} \right)^{\lambda-1} \cdot P \cdot Q \\ &\leq \left(q \cdot \frac{P \tilde{Q}}{\tilde{P} Q} + (1-q) \right)^{\lambda-1} \cdot \left(\frac{Q}{\tilde{Q}} \right)^{\lambda-1} \cdot P \cdot Q \\ &= \left(q \cdot \frac{P \tilde{Q}}{\tilde{P} Q} + (1-q) \right)^{\lambda-1} \cdot \left(\frac{Q}{\tilde{Q}} \right)^\lambda \cdot P \cdot \tilde{Q}, \end{aligned} \quad (\text{C.10})$$

where in the inequality we have used Lemma C.1. Now we can expand $\left(q \cdot \frac{P}{\tilde{P}} \frac{\tilde{Q}}{Q} + 1 - q\right)^{\lambda-1}$:

$$\begin{aligned}
\left(1 - q + q \cdot \frac{P}{\tilde{P}} \frac{\tilde{Q}}{Q}\right)^{\lambda-1} \cdot \left(\frac{Q}{\tilde{Q}}\right)^{\lambda} \cdot P \cdot \tilde{Q} &= \left(\sum_{j=0}^{\lambda-1} \binom{\lambda-1}{j} q^j \cdot (1-q)^{\lambda-1-j} \cdot \left(\frac{P}{\tilde{P}}\right)^j \left(\frac{\tilde{Q}}{Q}\right)^j\right) \cdot \left(\frac{Q}{\tilde{Q}}\right)^{\lambda} \cdot P \cdot \tilde{Q} \\
&= \left(\sum_{j=0}^{\lambda-1} \binom{\lambda-1}{j} q^j \cdot (1-q)^{\lambda-1-j} \cdot \left(\frac{P}{\tilde{P}}\right)^j \left(\frac{Q}{\tilde{Q}}\right)^{\lambda-j}\right) \cdot P \cdot \tilde{Q} \\
&= \sum_{j=0}^{\lambda-1} \binom{\lambda-1}{j} q^j \cdot (1-q)^{\lambda-1-j} \cdot \left(\frac{P}{\tilde{P}}\right)^{j+1} \tilde{P} \cdot \left(\frac{Q}{\tilde{Q}}\right)^{\lambda-j} \tilde{Q}.
\end{aligned}$$

Then, we use the known $\varepsilon_P(\lambda)$ and $\varepsilon_Q(\lambda)$ -values as in (C.9) to arrive at the claim. □

D f -Divergence of Parallel Compositions

We first formulate the parallel composition result for general f -divergences (Lemma D.1). We then obtain the RDP bound for parallel compositions as a corollary (Cor. D.2).

Our Lemma D.1 below can be seen as an f -divergence version of the $(\varepsilon, 0)$ -DP result given in (Thm. 4 McSherry, 2009). Corollary 2 by Smith et al. (2022) gives the corresponding result in terms of μ -Gaussian differential privacy (GDP), and it is a special case of our Lemma D.1 as μ -GDP equals the (ε, δ) -DP (i.e., the hockey-stick divergence) of the Gaussian mechanism with a certain noise scale (Cor. 1, Dong et al., 2022).

We define f -divergence for distributions on \mathbb{R}^d as follows. Consider two probability densities P and Q defined on \mathbb{R}^d , such that if $Q(x) = 0$ then also $P(x) = 0$, and a convex function $f : [0, \infty) \rightarrow \mathbb{R}$. Then, an f -divergence (Liese and Vajda, 2006) is defined as

$$D_f(P||Q) = \int f\left(\frac{P(t)}{Q(t)}\right) Q(t) dt.$$

In case the data is divided into disjoint shards and separate mechanisms are applied to each shard, the f -divergence upper bound for two neighbouring datasets can be obtained from the individual f -divergence upper bounds:

Lemma D.1. *Suppose a dataset $X \in \mathcal{X}^N$ is divided into k disjoint shards X_i , $i \in [k]$, and mechanisms \mathcal{M}_i , $i \in [k]$, are applied to the shards, respectively. Consider the mechanism*

$$\mathcal{M}(X) = (\mathcal{M}_1(X_1), \dots, \mathcal{M}_k(X_k)).$$

Then, we have that

$$\max_{X \sim Y} D_f(\mathcal{M}(X)||\mathcal{M}(Y)) \leq \max_{i \in [k]} \max_{X \sim Y} D_f(\mathcal{M}_i(X)||\mathcal{M}_i(Y)).$$

Proof. Let X be divided into k shards as described above and suppose Y is a neighbouring dataset such that $X_1 \sim Y_1$ and $Y = \{Y_1, X_2, \dots, X_k\}$.

Then, we see that

$$\begin{aligned} \frac{\mathbb{P}(\mathcal{M}(X) = (a_1, \dots, a_k))}{\mathbb{P}(\mathcal{M}(Y) = (a_1, \dots, a_k))} &= \frac{\mathbb{P}(\mathcal{M}_1(X_1) = a_1) \cdot \mathbb{P}(\mathcal{M}_1(X_2, a_1) = a_2) \cdots \mathbb{P}(\mathcal{M}_k(X_k, a_1, \dots, a_{k-1}) = a_k)}{\mathbb{P}(\mathcal{M}_1(Y_1) = a_1) \cdot \mathbb{P}(\mathcal{M}_1(X_2, a_1) = a_2) \cdots \mathbb{P}(\mathcal{M}_k(X_k, a_1, \dots, a_{k-1}) = a_k)} \\ &= \frac{\mathbb{P}(\mathcal{M}_1(X_1) = a_1)}{\mathbb{P}(\mathcal{M}_1(Y_1) = a_1)}. \end{aligned}$$

and furthermore, denoting $a = (a_1, \dots, a_k)$,

$$\begin{aligned} D_f(\mathcal{M}(X)||\mathcal{M}(Y)) &= \int f\left(\frac{\mathbb{P}(\mathcal{M}(X) = a)}{\mathbb{P}(\mathcal{M}(Y) = a)}\right) \mathbb{P}(\mathcal{M}(Y) = a) da \\ &= \int f\left(\frac{\mathbb{P}(\mathcal{M}_1(X_1) = (a_1))}{\mathbb{P}(\mathcal{M}_1(Y_1) = (a_1))}\right) \mathbb{P}(\mathcal{M}(Y) = a) da \\ &= \int f\left(\frac{\mathbb{P}(\mathcal{M}_1(X_1) = (a_1))}{\mathbb{P}(\mathcal{M}_1(Y_1) = (a_1))}\right) \mathbb{P}(\mathcal{M}(Y_1) = (a_1)) da_1 \\ &= D_f(\mathcal{M}_1(X_1)||\mathcal{M}_1(Y_1)). \end{aligned}$$

Thus,

$$D_f(\mathcal{M}(X)||\mathcal{M}(Y)) = D_f(\mathcal{M}_1(X_1)||\mathcal{M}_1(Y_1)) \leq \max_{X \sim Y} D_f(\mathcal{M}_1(X)||\mathcal{M}_1(Y)).$$

Similarly, if $X_i \sim Y_i$, $i = 2, \dots, k$ and

$$Y = (X_1, \dots, X_{i-1}, Y_i, X_{i+1}, \dots, X_k),$$

we see that

$$D_f(\mathcal{M}(X)||\mathcal{M}(Y)) = D_f(\mathcal{M}_i(X_i)||\mathcal{M}_i(Y_i)) \leq \max_{X \sim Y} D_f(\mathcal{M}_i(X)||\mathcal{M}_i(Y)).$$

Thus, we have that

$$\max_{X \sim Y} D_f(\mathcal{M}(X)||\mathcal{M}(Y)) = \max_{i \in [k]} \max_{X \sim Y} D_f(\mathcal{M}_i(X)||\mathcal{M}_i(Y)).$$

□

Corollary D.2. *Suppose a dataset $X \in \mathcal{X}^N$ is divided into k disjoint shards X_i , $i \in [k]$, and mechanisms \mathcal{M}_i , $i \in [k]$, are applied to the shards, respectively. Consider the mechanism*

$$\mathcal{M}(X) = (\mathcal{M}_1(X_1), \dots, \mathcal{M}_k(X_k)).$$

Suppose each \mathcal{M}_i is $(\lambda, \varepsilon_i(\lambda))$ -RDP, respectively. Then, \mathcal{M} is $(\lambda, \max_{i \in [k]} \varepsilon_i(\lambda))$ -RDP.

Proof. This follows from Lemma D.1 since

$$\exp((\lambda - 1)D_\lambda(\mathcal{M}(X)||\mathcal{M}(Y))) = \int \left(\frac{\mathbb{P}(\mathcal{M}(X) = a)}{\mathbb{P}(\mathcal{M}(Y) = a)} \right)^\lambda \mathbb{P}(\mathcal{M}(Y) = a) \, da$$

is an f -divergence for $f(x) = x^\lambda$. Thus, by Lemma D.1 we have that

$$\max_{X \sim Y} \exp((\lambda - 1)D_\lambda(\mathcal{M}(X)||\mathcal{M}(Y))) \leq \max_{i \in [k]} \max_{X \sim Y} \exp((\lambda - 1)D_\lambda(\mathcal{M}_i(X)||\mathcal{M}_i(Y)))$$

from which it follows that

$$\max_{X \sim Y} D_\lambda(\mathcal{M}(X)||\mathcal{M}(Y)) \leq \max_{i \in [k]} \max_{X \sim Y} D_\lambda(\mathcal{M}_i(X)||\mathcal{M}_i(Y)) = \max_{i \in [k]} \varepsilon_i(\lambda).$$

□

E Additional Experiments

E.1 Comparison of (ε, δ) -Bounds

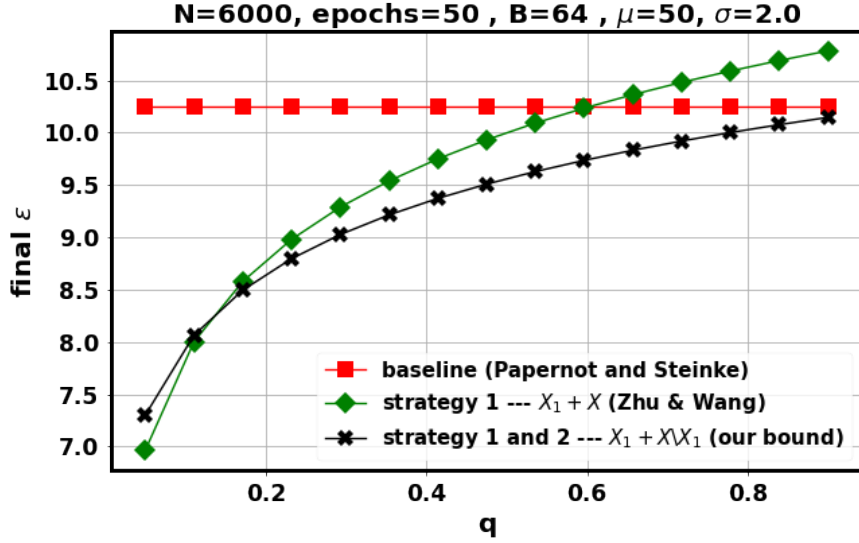


Figure 4: Final ε as a function of q for $\mu = 50$, when the base mechanism is the subsampled Gaussian mechanism with $\gamma = 64/6000$, number of epochs = 50 and $\sigma = 2.0$. The value of q varies from 0.05 to 0.9. Strategy 1 has considerably smaller ε 's for $q \leq 0.1$ compared to the baseline. However, with $q \leq 0.1$, strategy 1 may not provide good utility on small data sets (e.g., IMDB). Our proposed Thm. 7 used for the mechanism (3.1) ($X_1 + X \setminus X_1$) is suboptimal since for small values of q (e.g. $q = 0.05$) the bound of the mechanism (3.2) obtained with Thm. 4 is tighter.

E.2 Vary k in Strategy 2

For strategy 2, higher k 's provide more estimators in the ensemble. On the other hand, each submodel is trained on a shard of smaller size. To experimentally see the effect of k , we carry out an experiment similar to the one described in Section 5.1 for a different values of k . Figure 5 shows test accuracy as a function of target ε , k , and final ε for strategy 2. The value of k in each plot varies from 2 to 10. The first observation is that higher values of k reduce the final ε (at the cost of lower accuracy). This is due to smaller values of q ($q = \frac{1}{k}$) in Theorem 7. The $k = 2$ case generally yields the peak accuracy on all datasets, although in some cases higher k would have lead to better privacy-utility trade-off. We fix $k = 2$ in the experiments of the main text. In strategy 2, the compute cost of the tuning part also lowers the overall compute cost. Moreover, larger k 's reduce the training time for each submodel and the submodels can be trained in parallel.

E.3 Vary q in Strategy 1

In strategy 1, when q increases, the hyperparameter tuning mechanism trains with a larger dataset which means also weaker final privacy guarantees. Additionally, the best learning rate from the first model is also scaled with a smaller factor in the final model. We perform for strategy 1 an experiment similar as described in E.2 to compute the final test accuracies and ε -values as a function of q .

Figure 6 shows the test accuracy as a function of target ε for the base mechanism (DP-SGD), q , final ε . The value of q in each plot varies from 0.1 to 0.8. As expected, the accuracy for the variant that use $X \setminus X_1$ in the final model drops when q increases. The performance of the other variant that trains the final model with the full dataset remains relatively steady for all models. In IMDB, we use DP-Adam to train the IMDB model and do not scale the best initial learning rate.

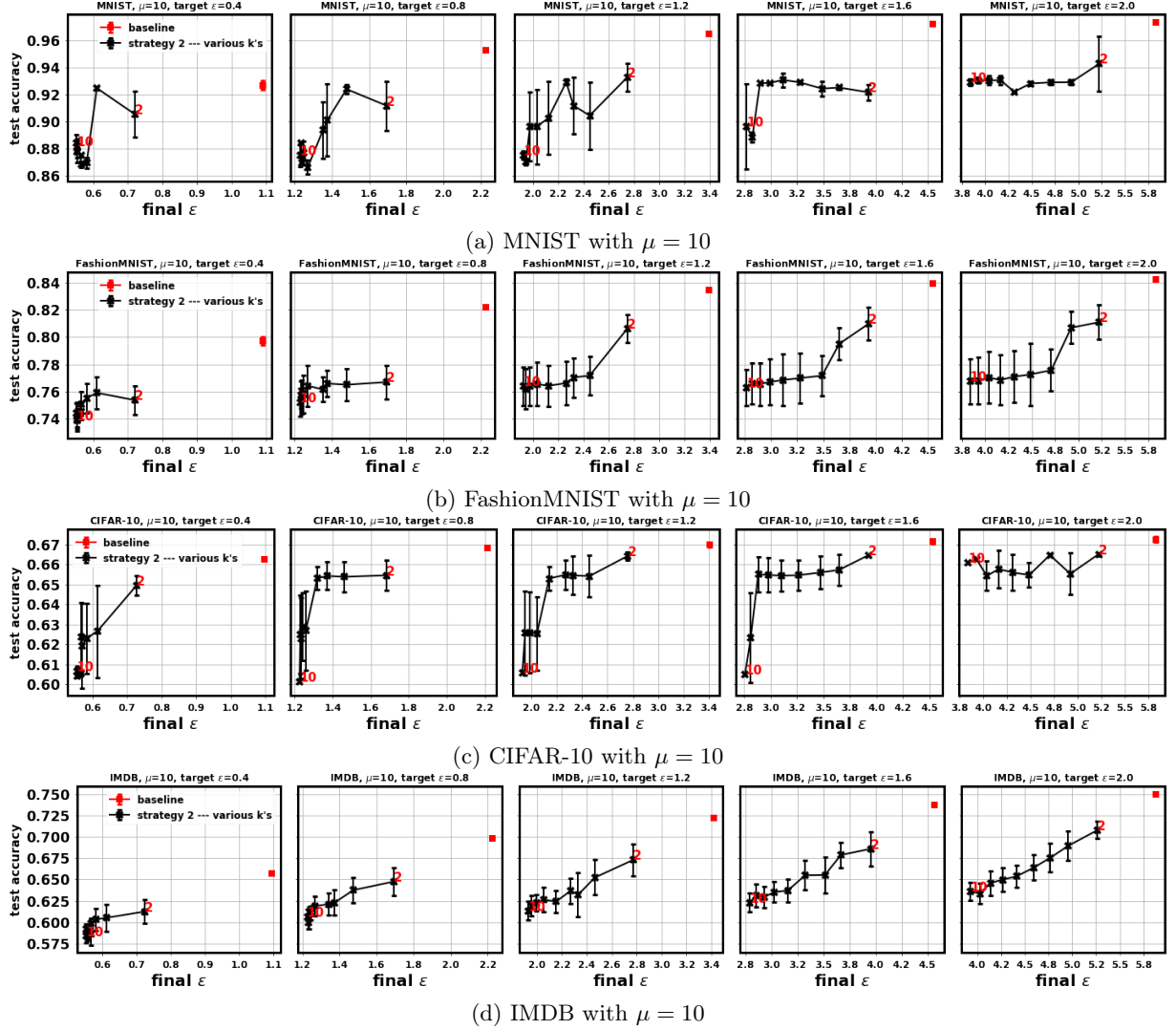


Figure 5: Tuning learning rate for strategy 2: We keep the batch size and the number of epochs fixed and only tune the learning rate, for various values of k . The test accuracies are averaged across 5 independent runs. The error bars denotes the std. error of the mean. Each plot contains 9 points for strategy 2, one for each $k \in \{2, 3, \dots, 10\}$ (right to left). We also add the baseline method for comparison. The $k = 2$ case generally yields the peak accuracy on all datasets.

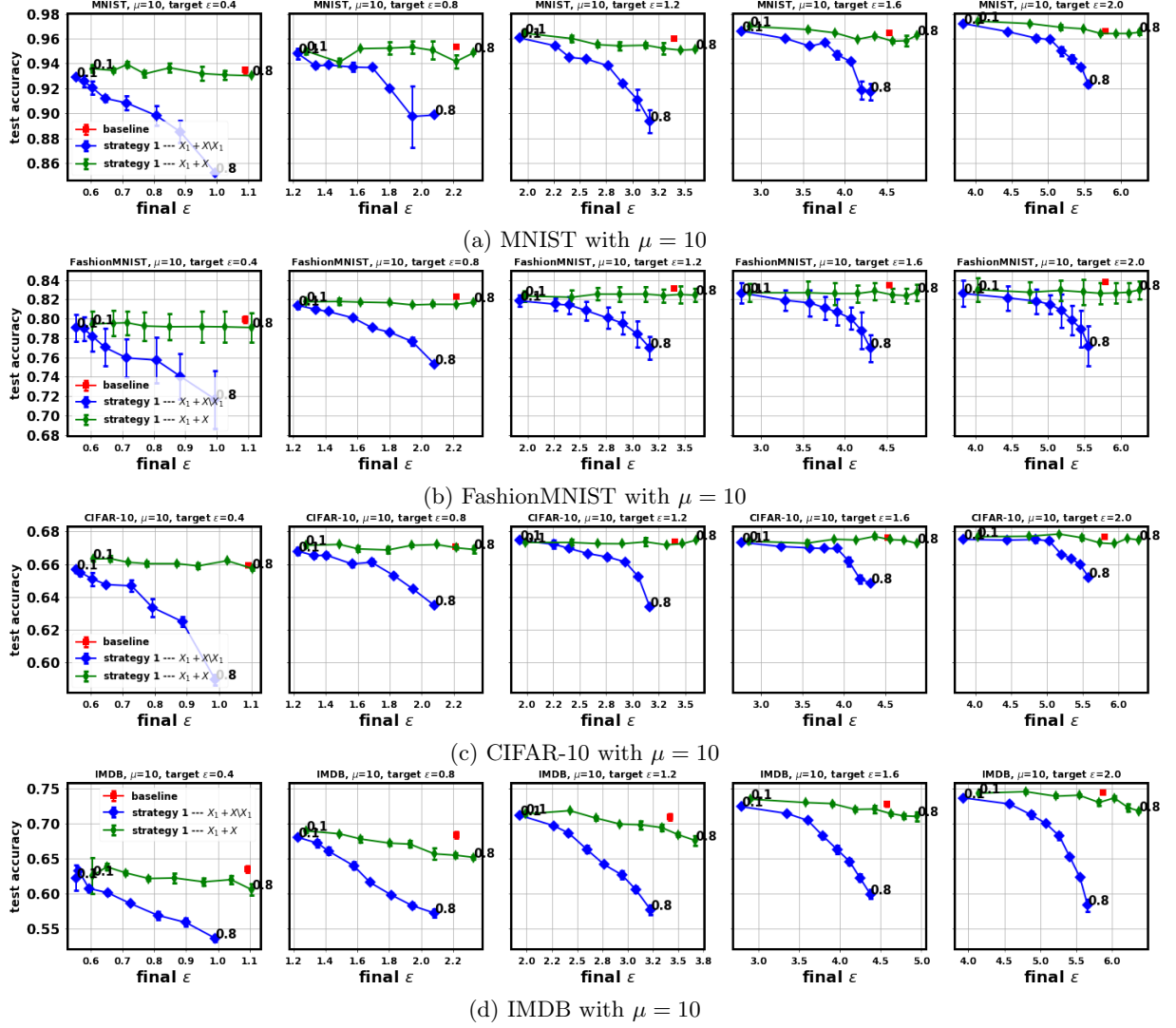


Figure 6: Tuning learning rate for strategy 1: We keep the batch size, the number of epochs fixed and only tune the learning rate for strategy 1 for various values of q . Test accuracies are averaged across 5 independent runs. The error bars denotes the std. error of the mean. Each plot contains 8 points for strategy 1, one for each $q \in \{0.1, 0.2, \dots, 0.8\}$ (left to right). We also add the baseline method for comparison. The $q = 0.1$ case generally yields the peak accuracy on all datasets.

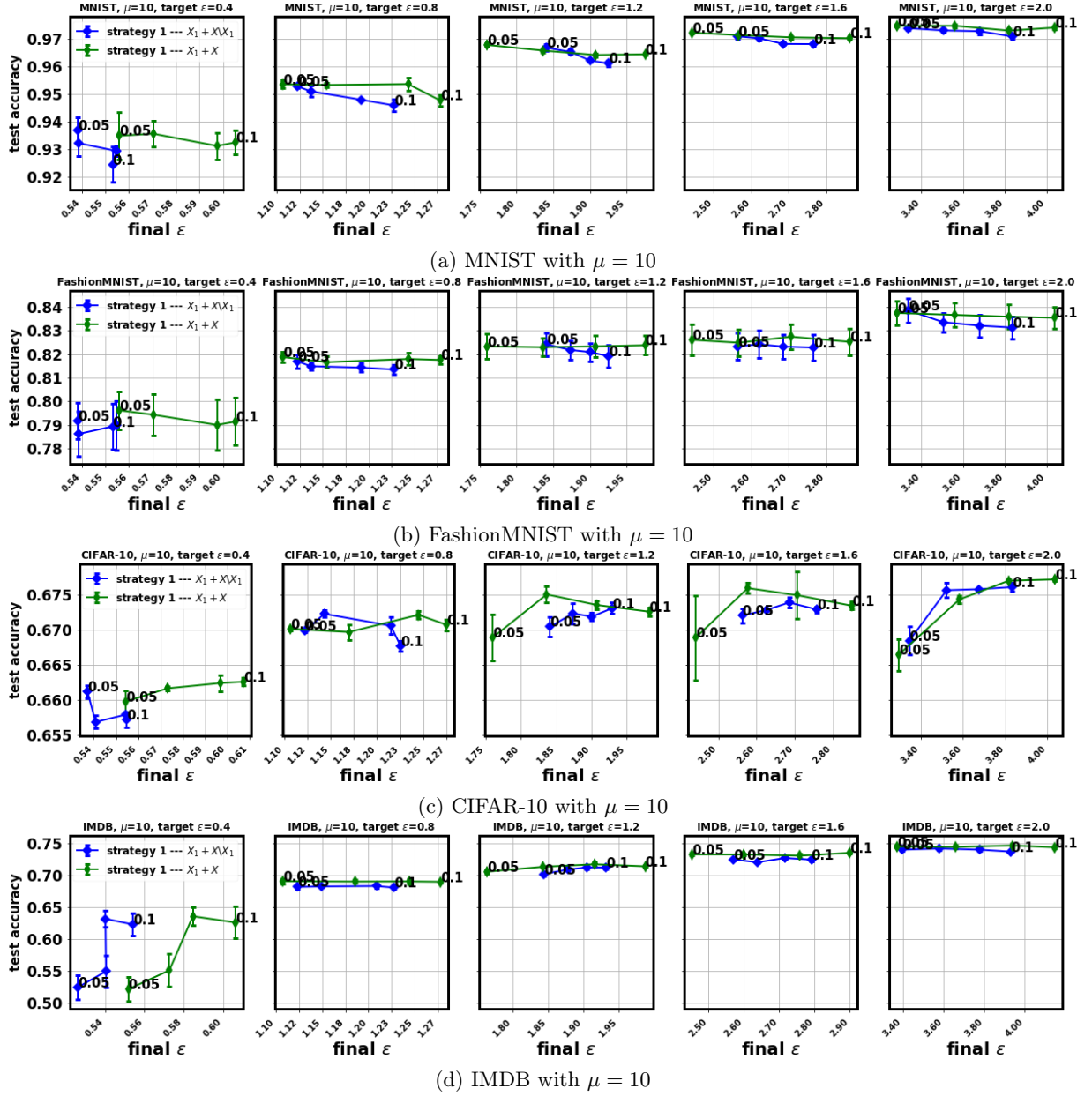


Figure 7: Tuning learning rate for strategy 1 for $q \leq 0.1$: We keep the batch size and the number of epochs fixed and only tune the learning rate for strategy 1 for various values of $q \leq 0.1$. Test accuracies are averaged across 5 independent runs. The error bars denotes the std. error of the mean. Each plot contains 4 points for strategy 1, i.e. when $q \in \{0.05, 0.067, 0.083, 0.1\}$. As shown in Fig. 4, the RDP bound of Thm. 7 is suboptimal and therefore the final ε -value for the variant of strategy 1 that uses the entire data is lower in some cases.